






# Galaxy And Mass Assembly: the xSAGA galaxy complement in nearby galaxy groups

B. W. Holwerda <sup>1</sup>★, S. Phillipps <sup>2</sup>★, S. Weerasooriya,<sup>3</sup> M. S. Bovill,<sup>3</sup> S. Brough <sup>4</sup>★, M. J. I. Brown <sup>5</sup>,  
C. Robertson <sup>1</sup> and K. Cook<sup>1</sup>

<sup>1</sup>Department of Physics and Astronomy, University of Louisville, Natural Science Building 102, Louisville, KY 40292, USA

<sup>2</sup>Astrophysics Group, School of Physics, University of Bristol, Tyndall Avenue, Bristol BS8 1TL, UK

<sup>3</sup>Department of Physics and Astronomy, Texas Christian University, Fort Worth, TX 76109, USA

<sup>4</sup>School of Physics, University of New South Wales, NSW 2052, Australia

<sup>5</sup>Monash Centre for Astrophysics (MoCA), School of Physics and Astronomy, Monash University, Clayton, VIC 3800, Australia

Accepted 2023 September 23. Received 2023 September 21; in original form 2023 June 24

## ABSTRACT

Groups of galaxies are the intermediate density environment in which much of the evolution of galaxies is thought to take place. In spectroscopic redshift surveys, one can identify these as close spatial-redshift associations. However, spectroscopic surveys will always be more limited in luminosity and completeness than imaging ones. Here, we combine the Galaxy And Mass Assembly (GAMA) group catalogue with the extended Satellites Around Galactic Analogues (xSAGA) catalogue of machine learning identified low-redshift satellite galaxies. We find 1825 xSAGA galaxies within the bounds of the GAMA equatorial fields ( $m_r < 21$ ), 1562 of which could have a counterpart in the GAMA spectroscopic catalogue ( $m_r < 19.8$ ). Of these, 1326 do have a GAMA counterpart with 974 below  $z = 0.03$  (true positives) and 352 above  $z = 0.03$  (false positives). By cross-correlating the GAMA group catalogue with the xSAGA catalogue, we can extend and characterize the satellite content of GAMA galaxy groups. We find that most groups have  $< 5$  xSAGA galaxies associated with them, but richer groups may have more. Each additional xSAGA galaxy contributes only a small fraction of the group's total stellar mass ( $\ll 10$  per cent). Selecting GAMA groups that resemble the Milky Way halo, with a few ( $< 4$ ) bright galaxies, we find that xSAGA can add a magnitude fainter sources to a group and that the Local Group does not stand out in the number of bright satellites. We explore the quiescent fraction of xSAGA galaxies in GAMA groups and find a good agreement with the literature.

**Key words:** galaxies: distances and redshifts – galaxies: general – galaxies: groups: general – Local Group – galaxies: photometry.

## 1 INTRODUCTION

Galaxies are social; most of them are found in groups of varying sizes (Eke et al. 2004; Robotham et al. 2011) and truly isolated individual galaxies are very rare (Alpaslan et al. 2014, 2015). The most extensive and massive systems are relatively easily identified in even a sparsely sampled redshift survey. However, small and compact groups are easily missed in such single-pass surveys, as fibre collisions prevent more than one group member making it into the catalogue (Robotham et al. 2010).

For groups of galaxies, an accurate redshift and thus distance and multiband photometry are essential to measure the stellar content and to infer to first order the group's halo mass from the ensemble's kinematics. However, *dynamical* masses need a measure of the velocity dispersion of such a group and hence one needs as many low-mass satellite galaxies (i.e. test masses in a dynamical system) as practical. Small groups are the most common but their dynamical mass (and hence dark matter content) is the least constrained from

kinematics. The best-studied example of such a group is the Local Group, the complex of the Milky Way, Andromeda, M33, and their subsidiary satellites. The central question is, however, how representative this Local Group is (e.g. in terms of galaxy occupation statistics; Boylan-Kolchin, Besla & Hernquist 2011; Lovell et al. 2011; Weisz et al. 2011; Robotham et al. 2014; Boylan-Kolchin et al. 2016). The make-up of the Local Group is still very much in development with lower mass and low surface brightness members still being discovered in deep imaging surveys (Bechtol et al. 2015; Drlica-Wagner et al. 2015, 2020; Kim et al. 2015; Koposov et al. 2015; Homma et al. 2019). See Simon (2019) for a review and Wang et al. (2021) for an overview of deep imaging results.

Here, our aim is to provide a context for the Local Group through statistics of the dynamical masses, including a census of satellites, similar to the Satellites Around Galactic Analogues (SAGA) project (Geha et al. 2017) but starting from the Galaxy And Mass Assembly (GAMA) group catalogue (Robotham et al. 2011) and supplementing it with machine learning (ML) identified satellites from the extended Satellites Around Galactic Analogues (xSAGA; Wu et al. 2022). We aim to verify the ML prediction in the xSAGA catalogue with a GAMA redshift where possible and to evaluate the properties of added xSAGA satellites to GAMA groups.

\* E-mail: [benne.holwerda@gmail.com](mailto:benne.holwerda@gmail.com) (BWH); [s.phillipps@bristol.ac.uk](mailto:s.phillipps@bristol.ac.uk) (SP); [s.brough@unsw.edu.au](mailto:s.brough@unsw.edu.au) (SB)

Cosmological Lambda cold dark matter ( $\Lambda$ CDM) simulations that attempt to reproduce galaxy groups (specifically the Local Group) struggle with not only the satellite distribution (e.g. satellite alignment; Hammer et al. 2013; Pawlowski, Kroupa & Jerjen 2013) but also the mass of the Magellanic Clouds (Benson et al. 2002; Kopolov et al. 2009; Okamoto et al. 2010). The simulations that match the Local Group’s properties require a very quiescent environment and a ‘quiet’, i.e. few mergers, assembly history of Andromeda and the Milky Way (Klypin, Zhao & Somerville 2002; Kravtsov 2002; Gottloeber, Hoffman & Yepes 2010; Forero-Romero et al. 2011). Reproducing the Local Group’s history from observed satellite populations is an active area of research and a touchstone test for cosmological simulations (Libeskind et al. 2011, 2020; Collins, Rich & Chapman 2012; Fattahi et al. 2013, 2016; Collins et al. 2014, 2016; Garrison-Kimmel et al. 2014, 2019a, b; Creasey et al. 2015; Sawala et al. 2016; Starkenburg et al. 2017; Elias et al. 2018; Digby et al. 2019). This all points to the possibility that the best-studied galaxy group with three massive members is – in fact – very unusual and not representative of the group environment in our Universe in which most galaxies reside. On the other hand, a sustained search for dwarf galaxy systems (Geha et al. 2012, 2017; Carlsten et al. 2021, 2022a, b; Mao et al. 2021; Wang et al. 2021) is showing that the Milky Way and M31 systems of satellites are not that unusual in their properties (e.g. fraction of quenched satellites).

Recently, the GAMA survey (Driver et al. 2011) has made great inroads into identifying smaller groups of galaxies reliably (Robotham et al. 2011, 2012, 2013, 2014). The impressive completeness of GAMA, 97 per cent of all  $r < 19.8$  magnitude sources in the field have spectroscopic redshifts (Liske et al. 2015; Driver et al. 2022), is enough to identify the lower mass galaxy groups reliably. For example, one can look for Local Group analogues, with up to three or four bright galaxies and many smaller ones. However, membership for the fainter galaxies remains uncertain because these typically do not have spectroscopic redshift measurements, even in the GAMA survey. Photometric redshift values are too uncertain: these cannot distinguish between distant background galaxies and faint group members.

A second development is the recent extension of the SAGA survey (Geha et al. 2017) by Wu et al. (2022) using ML classifications of faint galaxies to successfully classify these as either distant background or belonging to a single halo surrounding a Milky Way analogue (xSAGA). Here, we start with the GAMA group catalogue [GAMAGROUPS v10 from GAMA Data Release 4 (DR4)] and cross-correlate with the xSAGA catalogue to compare the number, size, colour, and surface brightness of xSAGA galaxies as a function of GAMA group properties.

This paper is organized as follows: Section 2 describes the GAMA group catalogue, Section 3 describes the xSAGA catalogue and the comparison with GAMA group positions, Section 4 describes the results of the comparison between the xSAGA and GAMA group catalogues, Section 5 discusses these results and places them in larger context with the aid of some group catalogues, and summarizes our results and conclusions. We assume a  $\Lambda$ CDM cosmology with the Planck18 cosmological parameters ( $H_0 = 67.4 \text{ km s}^{-1} \text{ Mpc}^{-1}$ ,  $\Omega_m = 0.315$ ; Planck Collaboration 2020).

## 2 GAMA GROUP SELECTION

Our starting point is the GAMA survey (Driver et al. 2009; Liske et al. 2015). GAMA is a highly complete ( $>97$  per cent to  $r < 19.8$  mag) spectroscopic and multiwavelength imaging survey conducted with the intent to investigate large-scale structure in the local Universe

( $z < 0.6$ ) on kpc to Mpc scales (Driver et al. 2009, 2011, 2022; Baldry et al. 2018). The survey now consists of five survey regions, three of which are equatorial, covering a total of nearly 250 000 galaxies. Additional photometric data were collected on each galaxy in 20+ bands at multiple wavelengths (Liske et al. 2015; Driver et al. 2016, 2022; Baldry et al. 2018). This specific study uses GAMA DR4, detailed in Driver et al. (2022). This highly complete redshift catalogue is ideal to identify smaller groupings of galaxies and local environments (Brough et al. 2011; Robotham et al. 2011, 2014). Robotham et al. (2011) constructed the galaxy group and pair catalogue using a friends-of-friends (FoF) algorithm.

From the Robotham et al. (2011) catalogue, updated for GAMA DR4 groups (GAMAGROUP v10), we select all galaxy groups with an FoF redshift centre below  $z = 0.03$ . This results in a selection of 272 groups. Fig. 1 shows their position on the sky. Fig. 2 shows the distribution of the number of GAMA galaxies in these groups. The majority of groups have two to three massive members in them, making them very similar to the Local Group.

## 3 XSAGA DWARF CATALOGUE

To quantify if a Milky Way analogue galaxy or a Local Group analogue has a similar retinue of satellite galaxies, one needs highly complete spectroscopic catalogues around every potential Milky Way + Andromeda grouping. In the local volume, this is the target for the ELVES survey (Carlsten et al. 2021, 2022b, a). For much larger volume searches, incompleteness plagues the accurate characterization of the retinue of satellite galaxies. Thus, a highly complete satellite catalogue has been the science objective of the SAGA (Geha et al. 2017) survey. However, this is observationally extremely expensive as it requires high-resolution spectroscopic redshift confirmation of intrinsically faint galaxies.

Wu et al. (2022) have produced a catalogue of dwarf galaxies based on the Dark Energy Spectroscopic Survey (DESI) imaging (Dey et al. 2019) using an ML technique. Their aim is to vastly expand the number of high-probability dwarf systems surrounding Local Group analogues. Wu et al. (2022) used the spectroscopic redshift catalogues of the SAGA survey to identify a training data set, and then optimized a convolutional neural network (CNN) to distinguish  $z < 0.03$  galaxies from more-distant objects using image cutouts from the DESI Legacy Imaging Surveys as input. Wu et al. (2022) identify a sample of over 100 000 CNN-selected low-redshift galaxies with CNN probabilities greater than 50 per cent to be located at low redshift ( $P_{z < 0.03} > 50$  per cent, Fig. 4). This is the extended SAGA catalogue (xSAGA). For xSAGA, Wu et al. (2022) claim to be complete to  $M_r < -15$  mag and select objects with  $m_r < 21$  mag. This is almost 1.5 mag deeper than the GAMA cut-off (Liske et al. 2015; Driver et al. 2022). This is the xSAGA catalogue against which we compare the low-redshift GAMA group positions and GAMA membership. GAMA was not used in the training of xSAGA and provides a completely independent confirmation of the CNN predictions by Wu et al. (2022). Redshift verification with GAMA spectroscopy of the ML low-redshift prediction is a first goal for this work.

### 3.1 xSAGA galaxies in GAMA

First, we examine how many xSAGA galaxies are in the equatorial survey area of GAMA (typically designated as the G09, G12, and G15 fields). Table 1 summarizes these numbers. We find that 1825 xSAGA galaxies are within these three fields RA and Dec. limits. Secondly, we compared the positions of xSAGA galaxies against

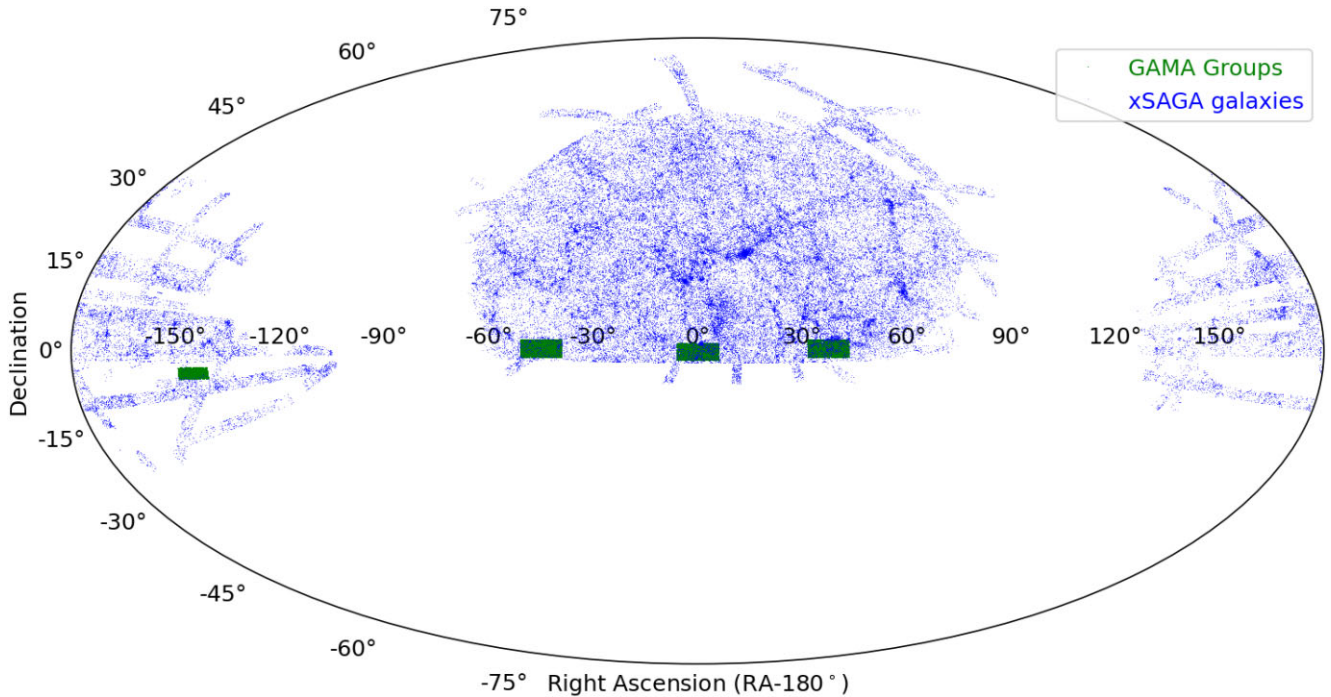


**Figure 1.** The position of the GAMA groups (green) and the xSAGA galaxies (blue). The GAMA equatorial fields (green rectangles in the middle) are complete and the best-studied ones. The GAMA group catalogue includes a fourth field, but this is not as complete in spectroscopic redshifts nor is it fully covered by xSAGA. For simplicity, we only analyse the equatorial fields here.

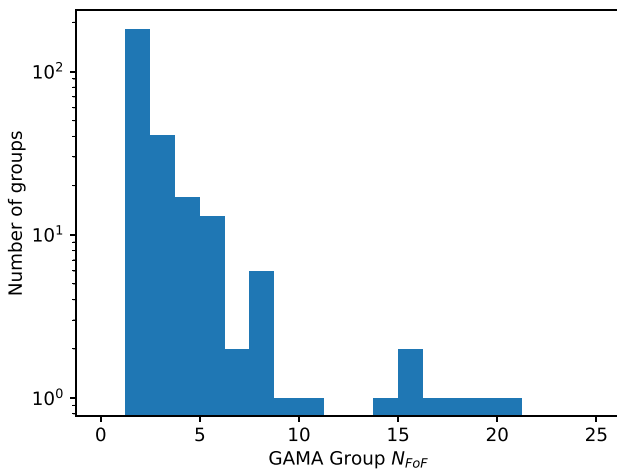


**Figure 2.** The number of galaxies in GAMA groups below  $z < 0.03$ . The majority are comprised of a few galaxies.

those of the GAMA catalogue (G3CGAL v10). Of the xSAGA galaxies in the equatorial fields, 1586 are bright enough to potentially be selected for GAMA ( $m_r = 19.8$ , 90 per cent complete; Driver et al. 2022). Of these possible GAMA members, 1326 have a counterpart in GAMA within 2 arcsec radius, the GAMA fibre aperture used on the Angle-Australian Telescope AAOmega instrument, 260 do not (84 per cent complete). The 6 per cent difference between the reported GAMA completeness and the one in xSAGA/GAMA overlap may be due to rejection of some xSAGA sources by their small angular size in the original GAMA target selection.

Fig. 3 shows the distribution of spectroscopic redshift and apparent magnitude for the xSAGA overlap with GAMA. The CNN

**Table 1.** The number of xSAGA galaxies in the equatorial fields, within the GAMA detection envelope, those found and not found in GAMA within the bounds of the equatorial fields and of those xSAGA galaxies with a counterpart in GAMA below and above the  $z = 0.03$  redshift limit that xSAGA was trained on.

Sample	Number of galaxies
xSAGA within three GAMA equatorial fields	1825
xSAGA within GAMA detection envelope (in equatorial fields, $m_r < 19.8$ )	1586
xSAGA within three GAMA equatorial fields not found in GAMA	260
xSAGA found in GAMA (in equatorial fields, $m_r < 19.8$ )	1326
xSAGA in GAMA below $z = 0.03$	974
xSAGA in GAMA above $z = 0.03$	352

probability assigned to each xSAGA galaxy is denoted by the colour for each point. Of the overlap of xSAGA and GAMA, 974 are below  $z = 0.03$  according to the GAMA spectroscopic redshift (true positives) and 352 are not (false positive). The false positive rate in the xSAGA/GAMA overlap is 26.5 per cent. The expectations from Wu et al. (2022) were for 71 per cent precision (purity or true positive rate) with a trailing of redshift values above  $z = 0.03$ . Wu et al. (2022) show in their fig. 3, how the CNN's precision declines below  $m_r = 19$  mag. Our true positive and false positive rates are consistent with the predicted true positive rate and the redshift behaviour and worsening performance at lower luminosities predicted by Wu et al. (2022).

It is not possible to estimate the true negative ( $T_N$ ) and false negative ( $F_N$ ) rates as we only have the xSAGA selection, not their

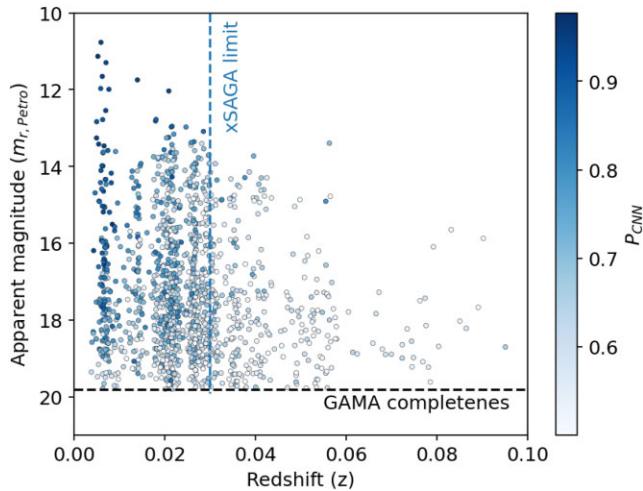


**Figure 3.** The redshift and  $r$ -band Petrosian apparent magnitude of xSAGA galaxies identified in the GAMA equatorial fields’ footprint with GAMA catalogue counterparts. The colour is indicative of the CNN confidence in the  $z < 0.03$  identification. Some 26.5 per cent are above the redshift limit and we note that the majority of these are lower confidence. A more stringent cut in CNN confidence level would result in a cleaner but less complete sample.

initial candidates. The precision<sup>1</sup> is 974/1326 (73 per cent), but for other typical metrics of ML, recall,<sup>2</sup> and the compound  $F1$  metric<sup>3</sup> we would need to know the true and false negative rates as well. The three metrics are often taken together as any ML algorithm is a trade-off between precise predictions and a complete selection from a large sample (recall). A precision metric over 70 per cent is perfectly workable in a statistical sense but individual sources and thus group membership have a substantial chance still of false positives.

In the following, we mark the galaxies that are common to xSAGA and GAMA in black and the new xSAGA candidate group members in blue.

### 3.2 Group cross-match

We only consider GAMA groups that are at redshifts below  $z < 0.03$  for cross-match. We adopt the  $r$ -band luminosity weighted centre of the group system as the position of the group centre. Starting from the group centre on the sky (CenRA, CenDec), we counted the numbers of xSAGA satellites within both R100 and R50, the full and half-radii of the group, and inferred the distance to the nearest xSAGA galaxy for each group using `MATCH_COORDINATES_SKY` in `ASTROPY.COORDINATES` to determine if they were within R100 or R50. In the case of groups of only two members, the full radius is the projected distance between them and the half-radius is half of that. The R100 radius is below the 300 kpc cut-off that Wu et al. (2022) use for group membership in training for almost all GAMA groups below  $z = 0.03$ . There are 272 GAMA groups in the group catalogue at redshifts below  $z = 0.03$ . Of these, 190 have one or more xSAGA galaxies associated with them within the R100 radius. Each GAMA

<sup>1</sup>Precision is defined as  $P = \left( \frac{T_P}{T_P + F_P} \right)$ , where  $T_P$  is the number of true positives and  $F_P$  is the number of false positives.

<sup>2</sup>Recall is defined as  $R = \left( \frac{T_P}{T_P + F_N} \right)$ , where  $T_P$  is the number of true positives and  $F_N$  is the number of false negatives.

<sup>3</sup>The  $F1$  metric is a combination of precision ( $P$ ) and recall ( $R$ ):  $F1 = 2 \times \left( \frac{P \times R}{P + R} \right)$ .

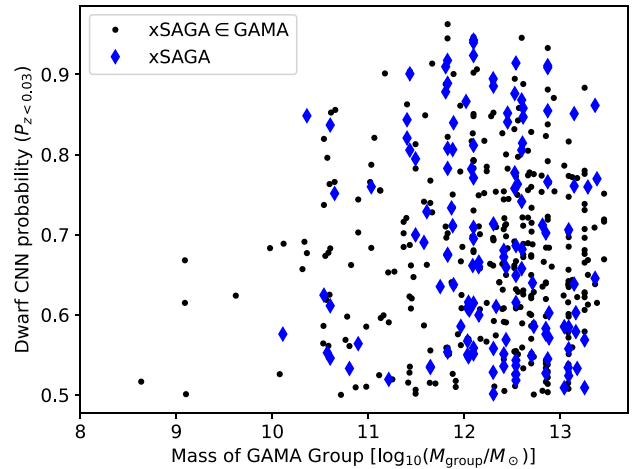


**Figure 4.** The CNN probability of an xSAGA galaxy being an  $z < 0.03$  galaxy as a function of its most likely associated GAMA group mass (MassA from the Robotham et al. 2011, catalogue). These are all the xSAGA galaxies down to  $m_r < 21$  and within the R100 of a GAMA group at  $z < 0.03$ . The few xSAGA galaxies in low-mass GAMA groups have CNN confidence levels in the lower range of acceptability compared to higher mass [ $\log_{10}(M/M_{\odot}) > 10.5$ ] groups.

group has a mass estimate (MassA) and total luminosity estimate (totRmag; Robotham et al. 2011). Fig. 4 shows the confidence level of the xSAGA CNN in the xSAGA galaxies associated with a GAMA group as a function of GAMA group mass. At the lower mass end of the GAMA groups [ $\log_{10}(M_{\text{group}}/M_{\odot}) < 10$ ], the xSAGA satellites are rarer and all already in GAMA. Above this group mass, there is no dependence on CNN confidence in the xSAGA identification on either group mass or selection as a GAMA target. xSAGA selection neither bias against group masses above this mass nor whether they were targeted by GAMA.

In the following, we compare the group characteristics, the number of galaxies in the group found via FoF, the dynamical mass of the group, and the total SDSS- $r$  band luminosity ( $N_{\text{FoF}}$ , MassA, totRmag), to those characteristics observed in the xSAGA satellites. MassA is used in the following figures as the mass of the GAMA group [ $\log_{10}(M_{\text{group}}/M_{\odot})$ ] and totRmag as the measure of group luminosity for an estimate of the total stellar mass in Section 4.3.

## 4 RESULTS

The results of this exercise to expand the satellite tally in GAMA groups using xSAGA catalogue can be split into a few broad categories: what we learned about the GAMA groups, what we learned about the satellite galaxy population now associated with galaxy groupings, and how our Local Group satellite population compares to other, similar groups in broader surveys.

### 4.1 Numbers of xSAGA satellites inside GAMA groups

Here, we look at the numbers of xSAGA galaxies that fall within a GAMA group’s boundary, either the half or full fraction of galaxies radius (R50 or R100). Fig. 5 shows the number of new xSAGA galaxies within the half-size and full-size radius of the group as a function of mass. The number of FoF identified GAMA galaxies in the group is indicated with the colour-bar. The majority of GAMA groups do not have an xSAGA satellite associated with them within

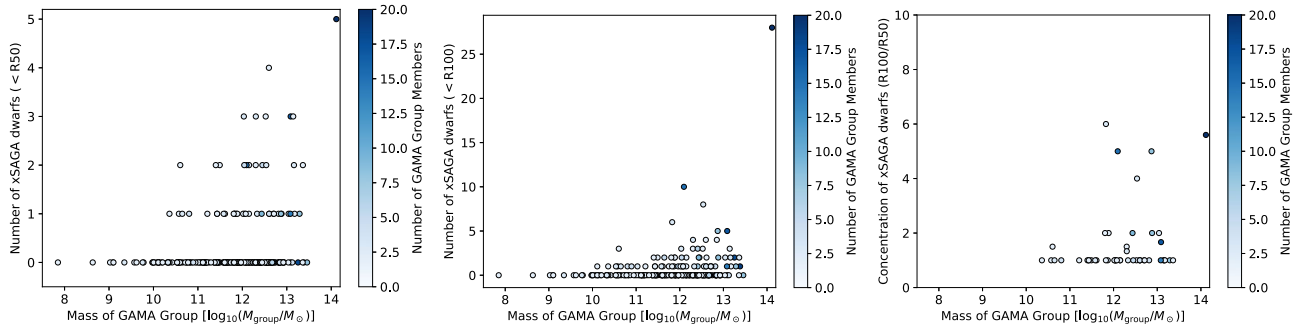


**Figure 5.** The number of new xSAGA galaxies found within the 50 per cent radius (left) and 100 per cent radius (middle) of each GAMA group as a function of GAMA group mass (MassA from the Robotham et al. 2011, catalogue). The concentration of new xSAGA candidate group members (right panel) is defined as the ratio of the number found within R100 divided by that within R50. Higher values of this ratio indicated a more spread-out satellite distribution within the R100 radius. Most groups concentrate their xSAGA retinue within R50, some have half within the R50, and the rest within the R100 radius. And only a few massive groups have the majority of their xSAGA satellites between R50 and R100. The one group at  $\log_{10}(M_{\text{group}}/M_{\odot}) \sim 14$  is both richer ( $N_{\text{FoF}} > 20$ ) and more enriched (27 xSAGA satellites within R100, middle panel). This could be considered a small cluster, rather than a sparse group.

either the R50 or R100. More massive groups, however, often have a few xSAGA identified satellites. There is one outlier of 25 xSAGA galaxies in a massive and rich group of 20 GAMA members. Fig. 5 shows the concentration of xSAGA ( $\notin$  GAMA) galaxies in groups, defined as follows:

$$C = \frac{N_{\text{xSAGA}}(< R100)}{N_{\text{xSAGA}}(< R50)}, \quad (1)$$

i.e. the ratio of the number of xSAGA galaxies within R100 over R50. Lower values of the concentration index means the new xSAGA galaxies are concentrated more towards the inner parts of the group. Higher values of this ratio indicated a more spread-out satellite distribution but within the R100 radius. Most groups retain their xSAGA retinue within R50, some have half within the R50 radius and the other half within full R100 (concentration of 2). And only a few massive groups have the majority of their xSAGA satellites between the R50 and R100 radii. Lower mass groups are more compact with their xSAGA satellites compared to more massive ones. Most GAMA groups are  $N = 2$  but some have up to 20 members and additionally show a wider distribution of associated xSAGA galaxies. We note a single massive group [ $\log_{10}(M_{\text{group}}/M_{\odot}) \sim 14$ , Group ID 200006] that is both richer ( $N_{\text{FoF}} = 67$ ) and more enriched (27 xSAGA satellites within R100). Generally speaking, an increase in the spatial distribution of satellites can be expected with increased group mass.

Fig. 6 shows the ratio of associated xSAGA galaxies to the total GAMA identified group members. A number of the more massive groups gain up to 200 per cent more members. This illustrates that a reliable ML search in images for fainter group members, such as the xSAGA project (Wu et al. 2022), will result in a plethora of new sources and potential targets for redshift measurements to improve the kinematic mass estimate for any galaxy groups identified through a few bright members in a spectroscopic redshift survey. The economy of an ML approach to this observational problem is cleanly illustrated here.

#### 4.2 xSAGA contribution to group stellar mass

How much additional stellar mass do these potential new members bring to the group? Figs 5 and 6 suggest a substantial contribution in number of galaxies to the groups. Here, we convert the  $g - r$  colour and SDSS- $r$  apparent magnitude reported for the xSAGA galaxies to a stellar mass using the prescription for stellar mass for the  $g$

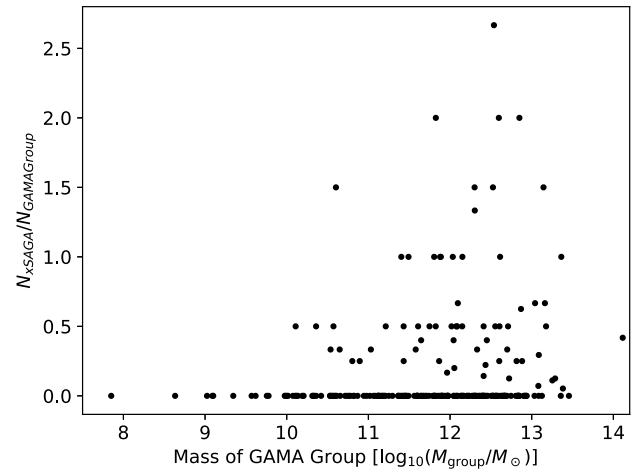


**Figure 6.** The ratio of the number of new xSAGA galaxies found within the 100 per cent radius of each GAMA group over the number of GAMA-defined group members as a function of GAMA group mass.

–  $r$  colour from Zibetti, Charlot & Rix (2009). We convert the total luminosity of the group in SDSS- $r$  band (from totRmag in the GAMA group catalogue, see Robotham et al. 2011) using the same colour for the SDSS- $r$  band M/L ratio. We thus arrive at a total group stellar mass and the stellar mass contribution by each xSAGA satellite.

Fig. 7 shows the fraction of stellar mass each xSAGA galaxy would have increased the group stellar mass by. The majority of the xSAGA galaxies already in GAMA contribute substantial fractions to the stellar mass of the group. Considering these are typically small groups, this is unsurprising. Most of the xSAGA galaxies not included in GAMA contribute a small fraction (less than 1 per cent of stellar mass) with some exceptions. The uncertainty on stellar mass contribution is substantial because we need to use a single colour to derive the mass-to-light ratio and the group’s distance to compute the absolute magnitude, when a GAMA redshift is not available. We note that xSAGA galaxies were associated with a group using projected radii. Even in the limited redshift range ( $z < 0.03$ , 136 Mpc), there could still be false positives i.e. foreground xSAGA galaxies included in a distant group or a background xSAGA galaxy included in a foreground galaxy group count. Even with a precision

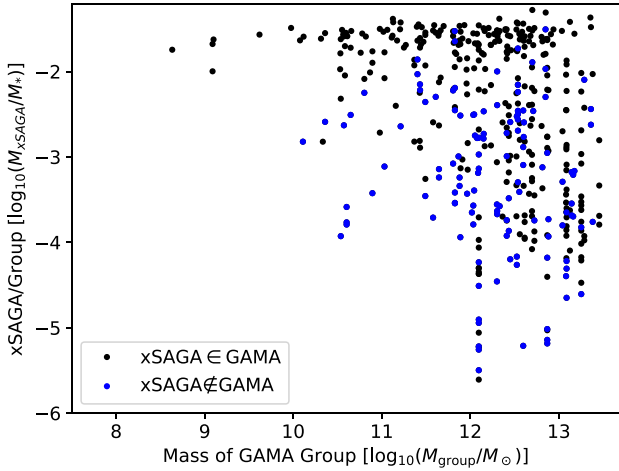


**Figure 7.** The fraction of the stellar mass that is contributed by xSAGA satellite galaxies to each GAMA group. Black dots are xSAGA galaxies with a GAMA counterpart and blue dots are without a GAMA catalogue counterpart.

of over 70 percent, a number of the additional satellites will be spurious.

For context, the intragroup light (IGL) of a single GAMA group [ $\log_{10}(M_{\text{group}}/M_{\odot}) \sim 13$ ] showed evidence for <36 percent of the group’s stellar mass in the diffuse IGL component (Martínez-Lombilla et al. 2023). A few per cent additional stellar mass fits the picture of slow present growth of the intragroup component if all these xSAGA satellites are eventually converted to the intragroup stellar population.

#### 4.3 xSAGA satellite characteristics in GAMA groups

In this section, we take a closer look at the characteristics of xSAGA satellites identified within the GAMA groups. Fig. 8 shows the effective surface brightness ( $\mu_{\text{eff}}$ ) of the xSAGA galaxies against the dynamical mass of the GAMA group (MassA). The effective surface brightness is computed from the  $r$ -band apparent magnitude ( $r_0$ ) and the effective radius by  $m_{r,\text{eff}} = r_0 + 2.5 \log [2\pi (R_{r,\text{eff}}/\text{arcsec})^2]$  (Wu et al. 2022). The effective radius ( $R_{r,\text{eff}}$ ) is the Petrosian  $r$ -band half-light radii, enclosing half the flux in the SDSS- $r$  band through a growth curve algorithm. The effective radii and effective surface brightness are from the DESI catalogue. xSAGA satellites’ surface brightnesses and small effective radii ( $r_{\text{eff}} \ll 10$  kpc) firmly put the majority of them in the lower surface brightness and dwarf galaxy regime. The symbols in Fig. 8 are colour-coded according to the  $g - r$  colour of the xSAGA galaxies. The colour scale is to highlight the separation between quiescent (red) and star-forming galaxies (blue) as defined by Salim et al. (2014). The majority of the xSAGA satellites is star forming but quiescent galaxies are picked up as well in all group masses. The selection of both red and blue galaxies by xSAGA shows that the initial colour selection and subsequent ML algorithm does not prohibitively bias against red galaxies.

#### 4.4 The quenched fraction of xSAGA satellites

The dependence of star formation on group environment was a key science goal for the GAMA project (see Driver et al. 2009). The general picture for *isolated* dwarf galaxies is that these almost all star forming (Haines et al. 2007; Geha et al. 2012; Kawinwanichakij

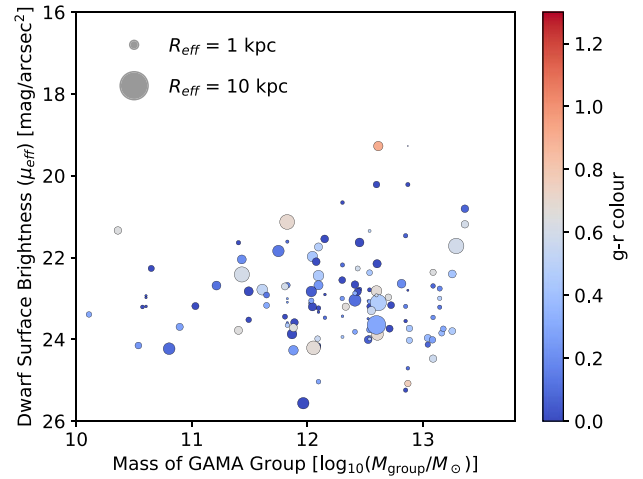


**Figure 8.** The surface brightness within the effective radius,  $g - r$  colour, and effective radius of the xSAGA galaxies not found in GAMA, found within the R100 radius of the GAMA groups as a function of GAMA group mass. The majority of xSAGA galaxies are small, within a small range of surface brightness, and of a range of  $g - r$  colour. The colour scale is to match the star-forming (blue) and quiescent (red) criterion of Salim et al. (2014). The majority of xSAGA galaxies are star forming but there is a substantial quiescent population.

et al. 2017) with only a small number of quiescent isolated galaxies reported (see Monachesi et al. 2014; Martínez-Delgado et al. 2016; Garling et al. 2020; Polzin et al. 2021; Casey et al. 2023). In GAMA groups, Treyer et al. (2017) examined the quenching of group central galaxies and found evidence for substantial quenching in satellites (‘conformity’, see also Weinmann et al. 2006; Wang & White 2012; Kauffmann et al. 2013). Grootes et al. (2017, 2018) found that gas cycling is similar to field spirals in the satellites of GAMA groups. They only find a lower specific star formation rate in the massive satellites. Sotillo-Ramos et al. (2021) find no evidence of quenching in groups for lower mass galaxies. Pearson et al. (2021) find that galaxies in groups typically become larger with group halo mass and no evidence for dramatic changes in morphology with increasing group mass. Davies et al. (2019a) note that scatter around the star formation and stellar mass relation does not follow the characteristic U-shape with stellar mass. Davies et al. (2019b) investigated the fraction of quiescent or passive galaxies in different mass ranges in more detail. They found a low fraction of passive/quenched galaxies at lower masses (5 percent at  $10^9 M_{\odot}$  for satellites). The general picture from GAMA for satellite galaxies is that they resemble field galaxies and any differences are subtle; the quenched fraction goes down with mass in both field and group satellite galaxies.

In Fig. 9, we show the stellar mass and specific star formation rates, inferred from full GAMA photometry (Wright et al. 2016; Driver et al. 2022) using MAGPHYS (da Cunha, Charlot & Elbaz 2008), of the GAMA galaxies that are in the xSAGA catalogue. The dashed line shows the cut-off between star forming and quiescent used in SAGA. Salim et al. (2014) compared quiescent/star-forming criteria and for the  $g - r$  colour, their fig. 4 shows a criterion at  $g - r = 0.65$ . This relation mostly holds for the xSAGA galaxies in GAMA and can be substituted in the xSAGA catalogue as a whole to distinguish between star-forming and quiescent populations.

Fig. 10 shows the fraction of quiescent/passive/quenched galaxies as a function of galaxy stellar mass for the xSAGA galaxies within the R100 radius of known GAMA groups that are similar to the Local

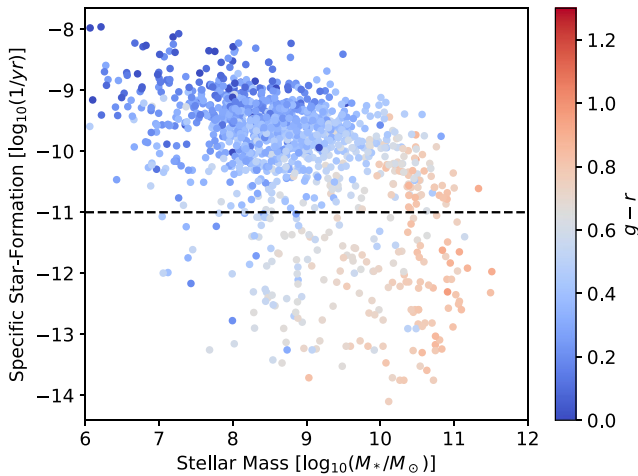


**Figure 9.** The stellar mass and star formation rate from MAGPHYS (da Cunha et al. 2008) spectral energy distribution fits of the GAMA full photometry (Wright et al. 2016; Driver et al. 2022) for the xSAGA galaxies in the GAMA survey. The fraction of star-forming galaxies is determined using the sSFR  $< -11 \text{ yr}^{-1}$  criterion, similar to xSAGA (Geha et al. 2017). The colour scale is the  $g - r$  colour from the xSAGA catalogue. The colour criterion ( $g - r = 0.65$ ) to separate star forming from quiescent in Salim et al. (2014) is similar but not an exact criterion.

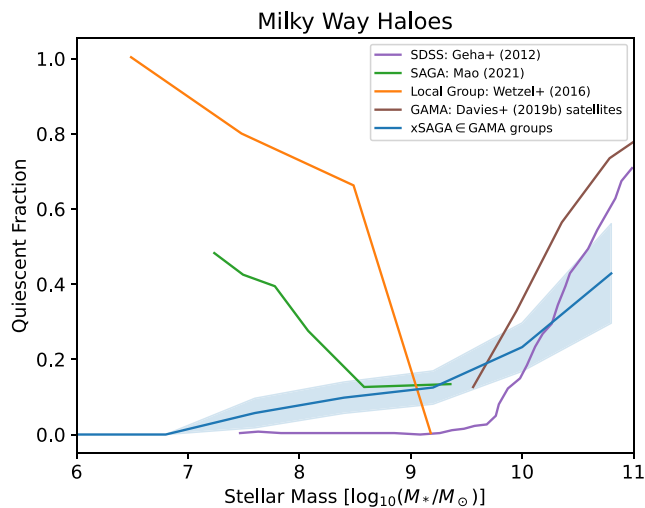


**Figure 10.** The fraction of quiescent xSAGA galaxies within the R100 of GAMA groups of similar mass as the Milky Way halo [ $\log_{10}(M_{\text{halo}}/M_{\odot}) = 12 - 12.4$ ]. An xSAGA galaxy is considered quiescent if the  $g - r$  colour is below 0.65 (Salim et al. 2014) and their stellar mass is inferred from the  $g - r$  colour, the group's redshift, and the apparent SDSS-r luminosity following the prescription in Zibetti et al. (2009). The quiescent fraction is very similar to the one found for GAMA satellites in Davies et al. (2019b).

Group halo. Fig. 10 shows for comparison the quiescent fractions from Sloan Digital Sky Survey (SDSS) (Geha et al. 2012), the SAGA survey (Mao et al. 2021), the Local Group (Wetzel et al. 2016), and all GAMA groups (Davies et al. 2019b).

The passive/quiescent fraction in xSAGA satellites follows the relation by Davies et al. (2019b) for GAMA groups for higher satellite galaxy masses [ $\log_{10}(M_*/M_{\odot}) > 10$ ] and the relation found by Geha et al. (2012). The lower mass galaxies have increasingly lower quiescent fractions. The useful limit of the early results (Geha et al. 2012; Davies et al. 2019b) is  $\log(M_*/M_{\odot}) = 9.5$ , below which

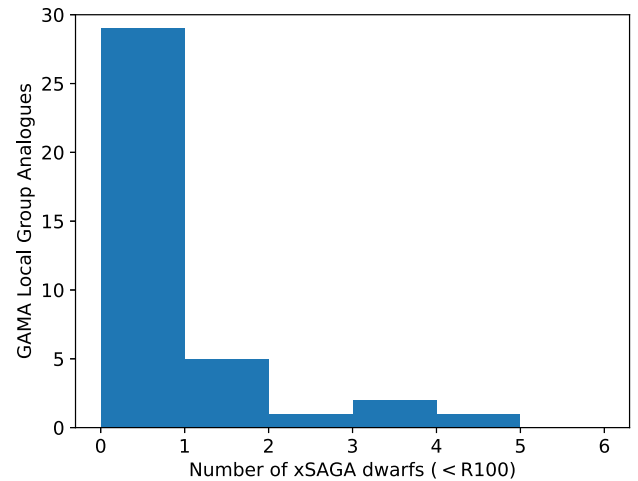


**Figure 11.** The histogram of the number of xSAGA galaxies, not included in GAMA ( $m_r < 21$ ), within the R100 radius of the 38 GAMA groups that resemble the Local Group [ $12 < \log_{10}(M_{\text{group}}) < 12.5$  and  $N_{\text{FoF}} < 4$ ]. Typical number of additional satellites is 1–2.

the surveyed population is not sufficient in size to determine a quiescent fraction. The Local Group mass function is complete to  $\log(M_*/M_{\odot}) = 6$  (Wetzel et al. 2016) and the targeted SAGA survey (Mao et al. 2021) to about  $\log(M_*/M_{\odot}) = 7$ . The xSAGA search in GAMA groups extends the mass limit down to  $\log(M_*/M_{\odot}) \sim 9$ .

The xSAGA passive fraction bridges to the SAGA passive fractions found at  $\log_{10}(M_*/M_{\odot}) \sim 9$ . Stellar mass for all xSAGA galaxies is derived using the M/L ratio from the  $g - r$  colour (Zibetti et al. 2009), the SDSS-r luminosity, and the associated group's redshift. Incompleteness increasingly plays a role at the lower mass range and Wu et al. (2022) note that their selection completeness and purity corrections are unconstrained below a stellar mass of  $\log_{10}(M_*/M_{\odot}) = 7.5$ . We note that xSAGA extends the useful range of GAMA for satellite quiescent fraction about an order of magnitude lower in stellar mass.

#### 4.5 Local Group equivalent xSAGA count

An extant problem in extragalactic research remains how typical the Local Group of galaxies is compared to other groups of galaxies. Fig. 11 shows the distribution of the number of xSAGA galaxies, not included in the GAMA galaxy catalogue but within the radius of GAMA groups that resemble the Local Group [ $12 < \log_{10}(M_{\text{group}}/M_{\odot}) < 12.5$  and  $N_{\text{FoF}} < 4$ ], where  $M_{\text{group}}$  is the dynamical mass and  $N_{\text{FoF}}$  is the number of members identified in the FoF algorithm. There are 38 GAMA groups that fit this criterion. The typical number of new small satellites identified by xSAGA appears to be 1–2.

Fig. 12 shows the luminosity function of new xSAGA galaxies within GAMA groups (xSAGA  $\notin$  GAMA), those xSAGA galaxies that are also in GAMA (xSAGA  $\in$  GAMA), and the luminosity function from McConnachie (2012) for the Local Group, both observed and limited to xSAGA observational limit. The xSAGA addition to GAMA groups allows one to examine the brightest satellites of Local Group analogues, thanks to the limiting magnitude of xSAGA ( $m_r = 21AB$  at  $z = 0.03$ , dashed vertical line). The addition of xSAGA allows for satellites, a magnitude fainter than GAMA to be included in group statistics. CNN projects like xSAGA will have

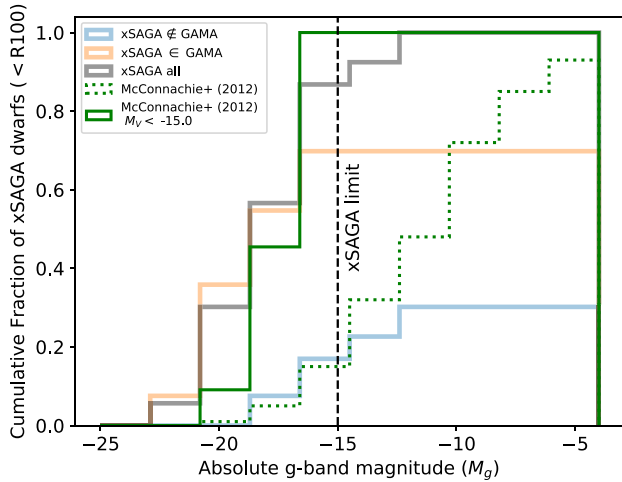


**Figure 12.** The cumulative histogram of the normalized number of xSAGA galaxies in GAMA groups that resemble the Local Group [ $12 < \log_{10}(M_{\text{group}}) < 12.5$  and  $N_{\text{FoF}} < 4$ , 28 unique GAMA groups with 53 xSAGA galaxies in total, 37 xSAGA  $\in$  GAMA, 16 xSAGA  $\notin$  GAMA] as a function of absolute SDSS-g magnitude. For those xSAGA galaxies included in GAMA (orange), we used the GAMA spectroscopic redshift for the distance modulus, and for those xSAGA galaxies not in GAMA (blue), we employed the group’s spectroscopic redshift ( $z_{\text{FoF}}$ ) for the distance modulus. The combined xSAGA number is shown as the thick grey line. For comparison, the relative Local Group satellite frequency as a function of V-band luminosity from McConnachie (2012) is shown in green. The observed luminosity function is shown as the dotted line and the cumulative distribution to  $M_{\text{lim}} = -15$  (dashed black vertical line), the limit of xSAGA is the solid green line. The Local Group has relatively fewer bright satellites compared to similar groups in GAMA. Close to the xSAGA limit, the Local Group is richer than the average GAMA group. We note that the completeness of xSAGA may play an important role ( $\sim 75$  per cent at  $M_{\text{lim}} = -15$ ; Wu et al. 2022).

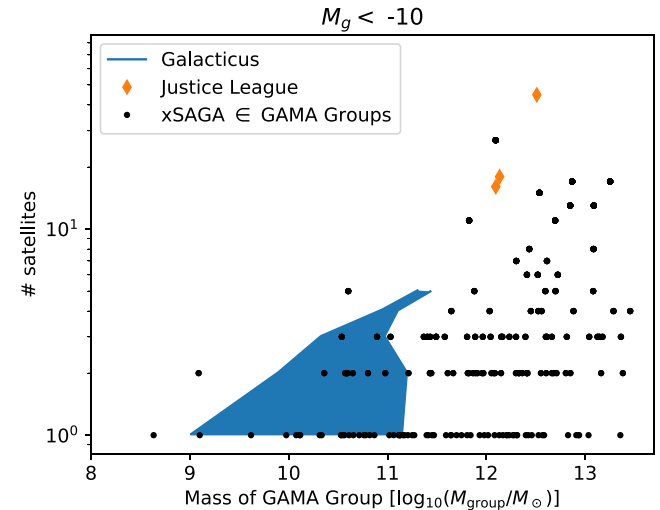
to be pushed to lower luminosities with future imaging surveys to fully probe the Local Group luminosity function.

Fig. 12 compares the Local Group relative numbers to those of similar dynamical mass and membership in GAMA using a cumulative, normalized histogram. We show the full range of Local Group luminosity function to illustrate the length current deep imaging and spectroscopic surveys still have to go before fully sampling a similar range in luminosities. Normalized over the total number of satellites found, the GAMA groups have relatively more bright satellites than the Local Group, the majority of which were already known in the GAMA catalogue ( $M_g < -17$ ). Adding xSAGA adds number at the intermediate absolute magnitudes ( $-17 < M_g < -13$ ). Because the xSAGA selection did not include a hard limiting magnitude, the number of xSAGA satellites added still rises beyond  $M_g = -15$ , hinting at the dimmer populations yet to be discovered and confirmed. The Local Group is very similar to these GAMA groups, when limited to the same absolute magnitude. The Kormogoriv-Smirnov and Anderson-Darling statistical test whether both luminosity functions above  $M_{\text{lim}} = -15$  are from the same parent distribution are inconclusive, i.e. the null hypothesis that both originate from the same distribution cannot be rejected with any confidence (see Table 2).

Previously, Guo et al. (2011) and Jiang, Jing & Li (2012) reported a factor 2 fewer extragalactic satellites than the average of MW and M31 satellites to a limit of  $M_V < -15$ , based on the SDSS and Canadian French Hawaiian Telescope (CFHT) imaging survey, respectively. However, Wang et al. (2021) concluded that the number

**Table 2.** The Kolmogorov–Smirnov (K–S) and Anderson–Darling (A–D) statistics of the satellite luminosity function of the Local Group and analogue groups with xSAGA satellites: those xSAGA galaxies already in GAMA, those xSAGA galaxies not in GAMA, and all combined. The number of xSAGA galaxies brighter than the limiting absolute magnitude is provided in parentheses.

Sample	No. of xSAGA galaxies ( $M_{\text{lim}} < -15$ )	K–S ( $p$ -value)	A–D statistic (sig. level)
xSAGA $\in$ GAMA	37 (36)	0.44 (0.05)	2.56 (0.03)
xSAGA $\notin$ GAMA	16 (7)	0.27 (0.83)	−0.33 (0.25)
xSAGA	53 (43)	0.37 (0.14)	1.90 (0.05)



**Figure 13.** The number of satellites in a virialized halo for the Galacticus (blue filled area; Benson 2012; Brennan et al. 2019; Bovill, private communication) and Justice League (orange diamond; Akins et al. 2021; Applebaum et al. 2021) simulations of group galaxies for satellites of absolute magnitudes of  $M_V < -10$  mag, the practical limit of xSAGA.

of satellites matches for Local Group analogues based on the HyperSuprimeCam, DECaLS, and SDSS imaging surveys. A logical following step is to expand the search for the lowest mass galaxies in nearby groups of galaxies (Tanaka et al. 2018; Mutlu-Pakdil et al. 2022), for example, the M81 grouping (Chiboucas et al. 2013; Monachesi et al. 2014) or the M101 (Danieli et al. 2017; Bennet et al. 2020; Garner et al. 2022) as nearby analogues for the Milky Way and its satellite retinue. Deeper imaging surveys have long held the promise to expand the satellite mass or luminosity functions of nearby galaxies (Tollerud et al. 2008; Danieli, van Dokkum & Conroy 2018; Wang et al. 2021); the Rubin Observatory certainly promises to do so (Mutlu-Pakdil et al. 2021). Once greater statistics are obtained on the satellite retinue of Milky Way/Local Group analogues (Busha et al. 2011; D’Souza et al. 2014), the Milky Way and its satellites can be placed in an evolutionary context (Lan, Ménard & Mo 2016; Danieli et al. 2023). Such group environment statistics can then be compared to, for example, completely isolated populations of low-mass galaxies (de los Reyes et al. 2023), to discern the effects of environment on low-mass galaxy evolution.

Fig. 13 shows the numbers of satellites in two suites of simulations, the semi-analytical Galacticus (Brennan et al. 2019; Weerasooriya et al. 2023) and smoothed particle hydrodynamical models of the Justice League (Akins et al. 2021; Applebaum et al. 2021)



for different luminosity cuts of the satellite population. The plot compares the results of the computationally expensive Justice League results to the much more computationally inexpensive Galacticus. The Justice League runs benefit from detailed physics at the highest resolutions presently run, while the Galacticus simulations can be thought of as a Local Group grounding of the prescriptions that make up semi-analytical models (Bovill et al., in preparation).

Fig. 13 shows the numbers of xSAGA galaxies – both those already in GAMA and new ones – with an absolute luminosity of  $M_g < -10$ , within the R100 radius for unique GAMA groups in our sample. The numbers are consistent for the intermediate mass groups [ $10 < \log_{10}(M_{\text{group}}/M_{\odot}) < 11$ ] with Galacticus but not for lower mass groups [ $\log_{10}(M_{\text{group}}/M_{\odot}) < 10$ ] for Galacticus. For the higher mass groups [ $\log_{10}(M_{\text{group}}/M_{\odot}) \sim 12$ ], the top satellite numbers agree well with the Justice League ones.

## 5 CONCLUSIONS

In this paper, we report a simple experiment where we compare the positions of very likely low-redshift ( $z < 0.03$ ,  $P_{z < 0.03} > 50$  per cent) galaxies identified with a CNN on DESI data (Wu et al. 2022) to the positions of galaxy groups identified in the GAMA survey using an FoF algorithm (Robotham et al. 2011, 2012). Exploring the number of likely low-redshift galaxies associated with GAMA groups, we find that the number of satellites associated with a GAMA group is between none and 5 for the majority of local GAMA groups. As can be expected, more massive and richer groups show a larger number of associated xSAGA satellites. Most of the associated xSAGA satellites span a range of surface brightness, are of intermediate colour ( $0 < g - r < 1$ ), and are small ( $R_{\text{eff}} < 10$  kpc). While the xSAGA galaxies add a number of new members to groups, their total stellar mass contribution to the group is very small: typically less than 1 per cent for the new xSAGA galaxies in a GAMA group.

We checked the redshifts of the xSAGA selection against the spectroscopic redshifts from GAMA and found a false positive rate of 30 per cent for the selection, consistent with Wu et al. (2022) predictions (Fig. 3). The xSAGA extension of the low-redshift GAMA groups constitutes a probabilistic extension to the group catalogue membership. This looks to be a promising approach to supplement high spectroscopic completeness surveys with probabilistic galaxy catalogues to attain an ever more complete picture of groups of galaxies, not just the retinue of Milky Way equivalent galaxies.

We compare the numbers of satellites found with xSAGA to group mass (Fig. 13) and these are in qualitative agreement with the Galacticus (Brennan et al. 2019) and Justice League (Akins et al. 2021; Applebaum et al. 2021) simulations of galaxy groups.

Selecting those GAMA groups that resemble the Local Group of galaxies [ $12 < \log_{10}(M_{\text{group}}/M_{\odot}) < 12.5$  and  $N_{\text{FoF}} < 4$ ], we find that such groups have a typical retinue of 1–2 xSAGA galaxies. The satellite luminosity function of Local Group analogue GAMA groups is quite similar to the one observed in the Local Group down to the equivalent limit of absolute luminosity for xSAGA (Fig. 12). Starting from those xSAGA galaxies that were included in GAMA observations, we explore the quiescent fraction of xSAGA galaxies as a function of stellar mass. This fraction is consistent with the one found in previous work (Geha et al. 2012; Davies et al. 2019b) but extends the useable range of stellar masses down to the SAGA surveys (Fig. 9).

In this paper, we show that the xSAGA extension using a CNN by Wu et al. (2022) is a very useful tool to expand a catalogue of known galaxy groups to lower stellar galaxy masses and we confirm independently the reported purity of the xSAGA sample (70 per cent)

with GAMA spectroscopic redshifts. The xSAGA expansion can be used for spectroscopic target pre-selection and statistical comparison between group memberships and simulations of galaxy groups.

## ACKNOWLEDGEMENTS

BWH would like to thank Karl Gordon for hosting him at STSCI, during which visit this idea crystallized. Special thanks to John Wu for making the xSAGA catalogue available and answering questions on his work.

## DATA AVAILABILITY

The GAMA DR4 (Driver et al. 2022) included v10 of the group catalogue GAMAGROUP v10 that describes the GAMA II equatorial and G02 survey regions. The full xSAGA satellite catalogue is not yet available but is expected to appear shortly.

## REFERENCES

- Akins H. B., Christensen C. R., Brooks A. M., Munshi F., Applebaum E., Engelhardt A., Chamberland L., 2021, *ApJ*, 909, 139
- Alpaslan M. et al., 2014, *MNRAS*, 440, L106
- Alpaslan M. et al., 2015, *MNRAS*, 451, 3249
- Applebaum E., Brooks A. M., Christensen C. R., Munshi F., Quinn T. R., Shen S., Tremmel M., 2021, *ApJ*, 906, 96
- Baldry I. K. et al., 2018, *MNRAS*, 474, 3875
- Bechtol K. et al., 2015, *ApJ*, 807, 50
- Bennet P., Sand D. J., Crnojević D., Spekkens K., Karunakaran A., Zaritsky D., Mutlu-Pakdil B., 2020, *ApJ*, 893, L9
- Benson A. J., 2012, *New Astron.*, 17, 175
- Benson A. J., Frenk C. S., Lacey C. G., Baugh C. M., Cole S., 2002, *MNRAS*, 333, 177
- Boylan-Kolchin M., Besla G., Hernquist L., 2011, *MNRAS*, 414, 1560
- Boylan-Kolchin M., Weisz D. R., Bullock J. S., Cooper M. C., 2016, *MNRAS*, 462, L51
- Brennan S., Benson A. J., Cyr-Racine F.-Y., Keeton C. R., Moustakas L. A., Pullen A. R., 2019, *MNRAS*, 488, 5085
- Brough S. et al., 2011, *MNRAS*, 413, 1236
- Busha M. T., Wechsler R. H., Behroozi P. S., Gerke B. F., Klypin A. A., Primack J. R., 2011, *ApJ*, 743, 117
- Carlsten S. G., Greene J. E., Greco J. P., Beaton R. L., Kado-Fong E., 2021, *ApJ*, 922, 267
- Carlsten S. G., Greene J. E., Beaton R. L., Greco J. P., 2022a, *ApJ*, 927, 44
- Carlsten S. G., Greene J. E., Beaton R. L., Danieli S., Greco J. P., 2022b, *ApJ*, 933, 47
- Casey K. J., Greco J. P., Peter A. H. G., Davis A. B., 2023, *MNRAS*, 520, 4715
- Chiboucas K., Jacobs B. A., Tully R. B., Karachentsev I. D., 2013, *AJ*, 146, 126
- Collins M. L. M., Rich R. M., Chapman S. C., 2012, in Aoki W., Ishigaki M., Suda T., Tsujimoto T., Arimoto N., eds, ASP Conf. Ser. Vol. 458, Galactic Archaeology: Near-Field Cosmology and the Formation of the Milky Way. Astron. Soc. Pac., San Francisco, p. 319
- Collins M. L. M. et al., 2014, *ApJ*, 783, 7
- Collins M. L. M., Rich R. M., Ibata R. A., Martin N. F., Preston J., 2016, in Gil de Paz A., Lee J. C., Knapen J. H., eds, Proceedings of IAU Symposium 321, 'Formation and evolution of galaxy outskirts'. Cambridge University Press, Cambridge Formation and Evolution of Galaxy Outskirts, p. 16
- Creasey P., Scannapieco C., Nuza S. E., Yepes G., Gottlöber S., Steinmetz M., 2015, *ApJ*, 800, L4
- da Cunha E., Charlot S., Elbaz D., 2008, *MNRAS*, 388, 1595
- Danieli S., van Dokkum P., Merritt A., Abraham R., Zhang J., Karachentsev I. D., Makarova L. N., 2017, *ApJ*, 837, 136
- Danieli S., van Dokkum P., Conroy C., 2018, *ApJ*, 856, 69

- Danieli S., Greene J. E., Carlsten S., Jiang F., Beaton R., Goulding A. D., 2023, *ApJ*, 956, 6
- Davies L. J. M. et al., 2019a, *MNRAS*, 483, 1881
- Davies L. J. M. et al., 2019b, *MNRAS*, 483, 5444
- de los Reyes M. A. C., Kirby E. N., Zhuang Z., Steidel C. C., Chen Y., Wheeler C., 2023, *ApJ*, 951, 52
- Dey A. et al., 2019, *AJ*, 157, 168
- Digby R. et al., 2019, *MNRAS*, 485, 5423
- Driver S. P. et al., 2009, *Astron. Geophys.*, 50, 050000
- Driver S. P. et al., 2011, *MNRAS*, 413, 971
- Driver S. P. et al., 2016, *ApJ*, 827, 108
- Driver S. P. et al., 2022, *MNRAS*, 513, 439
- Drlica-Wagner A. et al., 2015, *ApJ*, 813, 109
- Drlica-Wagner A. et al., 2020, *ApJ*, 893, 47
- D'Souza R., Kauffman G., Wang J., Vegetti S., 2014, *MNRAS*, 443, 1433
- Eke V. R. et al., 2004, *MNRAS*, 355, 769
- Elias L. M., Sales L. V., Creasey P., Cooper M. C., Bullock J. S., Rich R. M., Hernquist L., 2018, *MNRAS*, 479, 4004
- Fattahi A., Navarro J. F., Starkenburg E., Barber C. R., McConnachie A. W., 2013, *MNRAS*, 431, L73
- Fattahi A. et al., 2016, *MNRAS*, 457, 844
- Forero-Romero J. E., Hoffman Y., Yepes G., Gottlöber S., Piontek R., Klypin A., Steinmetz M., 2011, *MNRAS*, 417, 1434
- Garling C. T., Peter A. H. G., Kochanek C. S., Sand D. J., Crnojević D., 2020, *MNRAS*, 492, 1713
- Garner R., Mihos J. C., Harding P., Watkins A. E., McGaugh S. S., 2022, *ApJ*, 941, 182
- Garrison-Kimmel S., Boylan-Kolchin M., Bullock J. S., Kirby E. N., 2014, *MNRAS*, 444, 222
- Garrison-Kimmel S. et al., 2019a, *MNRAS*, 487, 1380
- Garrison-Kimmel S. et al., 2019b, *MNRAS*, 489, 4574
- Geha M., Blanton M. R., Yan R., Tinker J. L., 2012, *ApJ*, 757, 85
- Geha M. et al., 2017, *ApJ*, 847, 4
- Gottlöber S., Hoffman Y., Yepes G., 2010, *Proceedings of "High Performance Computing in Science and Engineering, Garching/Munich 2009"*. Springer-Verlag
- Grootes M. W. et al., 2017, *AJ*, 153, 111
- Grootes M. W. et al., 2018, *MNRAS*, 477, 1015
- Guo Q., Cole S., Eke V., Frenk C., 2011, *MNRAS*, 417, 370
- Haines C. P., Gargiulo A., La Barbera F., Mercurio A., Merluzzi P., Busarello G., 2007, *MNRAS*, 381, 7
- Hammer F., Yang Y., Fouquet S., Pawlowski M. S., Kroupa P., Puech M., Flores H., Wang J., 2013, *MNRAS*, 431, 3543
- Homma D. et al., 2019, *PASJ*, 71, 94
- Jiang C. Y., Jing Y. P., Li C., 2012, *ApJ*, 760, 16
- Kauffmann G., Li C., Zhang W., Weinmann S., 2013, *MNRAS*, 430, 1447
- Kawinwanichakij L. et al., 2017, *ApJ*, 847, 134
- Kim D., Jerjen H., Mackey D., Da Costa G. S., Milone A. P., 2015, *ApJ*, 804, L44
- Klypin A., Zhao H., Somerville R. S., 2002, *ApJ*, 573, 597
- Koposov S. E., Yoo J., Rix H.-W., Weinberg D. H., Macciò A. V., Escudé J. M., 2009, *ApJ*, 696, 2179
- Koposov S. E., Belokurov V., Torrealba G., Evans N. W., 2015, *ApJ*, 805, 130
- Kravtsov V., 2002, *A&A*, 396, 117
- Lan T.-W., Ménard B., Mo H., 2016, *MNRAS*, 459, 3998
- Libeskind N. I., Knebe A., Hoffman Y., Gottlöber S., Yepes G., Steinmetz M., 2011, *MNRAS*, 411, 1525
- Libeskind N. I. et al., 2020, *MNRAS*, 498, 2968
- Liske J. et al., 2015, *MNRAS*, 452, 2087
- Lovell M. R., Eke V. R., Frenk C. S., Jenkins A., 2011, *MNRAS*, 413, 3013
- McConnachie A. W., 2012, *AJ*, 144, 4
- Mao Y.-Y., Geha M., Wechsler R. H., Weiner B., Tollerud E. J., Nadler E. O., Kallivayalil N., 2021, *ApJ*, 907, 85
- Martínez-Delgado D. et al., 2016, *AJ*, 151, 96
- Martínez-Lombilla C. et al., 2023, *MNRAS*, 518, 1195
- Monachesi A. et al., 2014, *ApJ*, 780, 179
- Mutlu-Pakdil B. et al., 2021, *ApJ*, 918, 88
- Mutlu-Pakdil B. et al., 2022, *ApJ*, 926, 77
- Okamoto T., Frenk C. S., Jenkins A., Theuns T., 2010, *MNRAS*, 406, 208
- Pawlowski M. S., Kroupa P., Jerjen H., 2013, *MNRAS*, 435, 1928
- Pearson W. J., Wang L., Brough S., Holwerda B. W., Hopkins A. M., Loveday J., 2021, *A&A*, 646, A151
- Planck Collaboration, 2020, *A&A*, 641, A6
- Polzin A., van Dokkum P., Danieli S., Greco J. P., Romanowsky A. J., 2021, *ApJ*, 914, L23
- Robotham A. et al., 2010, *Publ. Astron. Soc. Aust.*, 27, 76
- Robotham A. S. G. et al., 2011, *MNRAS*, 416, 2640
- Robotham A. S. G. et al., 2012, *MNRAS*, 424, 1448
- Robotham A. S. G. et al., 2013, *MNRAS*, 431, 167
- Robotham A. S. G. et al., 2014, *MNRAS*, 444, 3986
- Salim S., Lee J. C., Ly C., Brinchmann J., Davé R., Dickinson M., Salzer J. J., Charlot S., 2014, *Serb. Astron. J.*, 189, 1
- Sawala T. et al., 2016, *MNRAS*, 457, 1931
- Simon J. D., 2019, *ARA&A*, 57, 375
- Sotillo-Ramos D. et al., 2021, *MNRAS*, 508, 1817
- Starkenburg E., Oman K. A., Navarro J. F., Crain R. A., Fattahi A., Frenk C. S., Sawala T., Schaye J., 2017, *MNRAS*, 465, 2212
- Tanaka M., Chiba M., Hayashi K., Komiyama Y., Okamoto T., Cooper A. P., Okamoto S., Spitler L., 2018, *ApJ*, 865, 125
- Tollerud E. J., Bullock J. S., Strigari L. E., Willman B., 2008, *ApJ*, 688, 277
- Treyer M. et al., 2017, *MNRAS*, 477, 2684
- Wang W., White S. D. M., 2012, *MNRAS*, 424, 2574
- Wang W. et al., 2021, *MNRAS*, 500, 3776
- Weerasooriya S., Bovill M. S., Benson A., Musick A. M., Ricotti M., 2023, *ApJ*, 948, 87
- Weinmann S. M., van den Bosch F. C., Yang X., Mo H. J., 2006, *MNRAS*, 366, 2
- Weisz D. R. et al., 2011, *ApJ*, 743, 8
- Wetzell A. R., Hopkins P. F., Kim J.-h., Faucher-Giguere C.-A., Keres D., Quataert E., 2016, *ApJL*, 827, L23
- Wright A. H. et al., 2016, *MNRAS*, 460, 765
- Wu J. F. et al., 2022, *ApJ*, 927, 121
- Zibetti S., Charlot S., Rix H., 2009, *MNRAS*, 400, 1181

This paper has been typeset from a  $\text{\TeX}/\text{\LaTeX}$  file prepared by the author.